



Synthesis and luminescence properties of $\text{Ba}_2\text{Gd}_2\text{Si}_4\text{O}_{13}:\text{Ce}^{3+}$ phosphor for UV light-emitting diodes



Cheng Yue, Wanrong Wang, Qingping Wang, Ye Jin*

School of Optoelectronic Information, Chongqing University of Technology, 69 Hongguang Street, Chongqing, 400054, China

ARTICLE INFO

Article history:

Received 16 March 2016

Received in revised form

27 April 2016

Accepted 11 May 2016

Available online 13 May 2016

Keywords:

$\text{Ba}_2\text{Gd}_2\text{Si}_4\text{O}_{13}:\text{Ce}^{3+}$

LED

Blue phosphor

Energy transfer

Optical materials and properties

Thermal analysis

ABSTRACT

The Ce^{3+} -doped $\text{Ba}_2\text{Gd}_2\text{Si}_4\text{O}_{13}$ was synthesized by solid-state reaction. Under excitation at 329 nm, the PL spectra of $\text{Ba}_2\text{Gd}_2\text{Si}_4\text{O}_{13}:\text{Ce}^{3+}$ phosphors show a broad band peaking at 396 nm, which is attributed to the spin-allowed 5d-4f transition of Ce^{3+} ions. The concentration quenching occurs at 6% in $\text{Ba}_2\text{Gd}_2\text{Si}_4\text{O}_{13}:\text{Ce}^{3+}$ and the critical energy transfer distance for Ce^{3+} in $\text{Ba}_2\text{Gd}_2\text{Si}_4\text{O}_{13}$ is calculated to be 16.56 Å, ascribing to dipole–dipole interaction. Thermal quenching comparison between $\text{Ba}_2\text{Gd}_2\text{Si}_4\text{O}_{13}:\text{Ce}^{3+}$ and $\text{BaMgAl}_{10}\text{O}_{17}:\text{Eu}^{2+}$ is investigated and the thermal quenching temperature $T_{0.5}$ is about 300 °C for $\text{Ba}_2\text{Gd}_2\text{Si}_4\text{O}_{13}:\text{Ce}^{3+}$. The chromaticity coordinates (x, y) of $\text{Ba}_2\text{Gd}_2\text{Si}_4\text{O}_{13}:\text{Ce}^{3+}$ are calculated to be (0.1584, 0.0285) with the CCT of 1886 K. The current result suggested that $\text{Ba}_2\text{Gd}_2\text{Si}_4\text{O}_{13}:\text{Ce}^{3+}$ is a potential blue phosphor for white-LEDs.

© 2016 Elsevier B.V. All rights reserved.

1. Introduction

Recently, white light emitting diodes (WLEDs) have been considered to be the fourth generation solid-state lighting because of their low energy consumption, high luminous efficiency, small volume, no pollution, and long life etc. [1–4] The current commercial white LED devices is main the combination InGaN blue LED chip with yellow $\text{Y}_3\text{Al}_5\text{O}_{12}:\text{Ce}^{3+}$ phosphors [1,5]. However, this WLEDs emits cool white with higher color temperature (CCT \approx 7750 K) and low color rendering index (CRI \approx 70–80) due to the lack of red [3,6,7]. In order to overcome these deficiencies, near ultraviolet LED chip with tricolor phosphors have been studied due to the excellent color rendering [8,9]. Therefore, it is necessary to develop blue, green and red emitting phosphors for near ultraviolet LED.

As an important family of luminescent materials, the silicates have drawn much attention as effective host lattices due to their good thermal stability, chemical stability, and strong water tolerance [10,11]. Wierzbicka-Wieczorek et al. first reported the silicate $\text{Ba}_2\text{Gd}_2\text{Si}_4\text{O}_{13}$ in 2010 [12]. In 2015, we reported the luminescent properties of $\text{Ba}_2\text{Gd}_2\text{Si}_4\text{O}_{13}:\text{Eu}^{2+}$ [13]. Nevertheless, the detailed

research on $\text{Ba}_2\text{Gd}_2\text{Si}_4\text{O}_{13}:\text{Ce}^{3+}$, such as the energy dispersive mechanism and thermal quenching properties, has not been done. Therefore, we synthesized a series of $\text{Ba}_2\text{Gd}_2\text{Si}_4\text{O}_{13}:\text{Ce}^{3+}$ samples via a solid-state reaction here. Simultaneously, the photoluminescence (PL) properties have been studied systematically. The concentration quenching occurs at 6% and the critical energy transfer distance for Ce^{3+} in $\text{Ba}_2\text{Gd}_2\text{Si}_4\text{O}_{13}$ is calculated to be 16.56 Å due to dipole–dipole interaction. Thermal quenching comparison between $\text{Ba}_2\text{Gd}_2\text{Si}_4\text{O}_{13}:\text{Ce}^{3+}$ and $\text{BaMgAl}_{10}\text{O}_{17}:\text{Eu}^{2+}$ is investigated and the thermal quenching temperature $T_{0.5}$ is about 300 °C for $\text{Ba}_2\text{Gd}_2\text{Si}_4\text{O}_{13}:\text{Ce}^{3+}$ phosphor. The results show that $\text{Ba}_2\text{Gd}_2\text{Si}_4\text{O}_{13}:\text{Ce}^{3+}$ has good prospect for WLEDs.

2. Experimental

2.1. Materials and synthesis

$\text{Ba}_2\text{Gd}_2\text{Si}_4\text{O}_{13}:\text{xCe}^{3+}$ (x = 0.01, 0.02, 0.04, 0.06 and 0.07) were synthesized via a high-temperature solid-state reaction. The raw materials were BaCO_3 (A.R.), SiO_2 (A.R.), Gd_2O_3 (99.9%), CeO_2 (99.99%). They were weighted on stoichiometric ratio then mixed together. The mixed powder was grounded for hours in an agate mortar. Then the ground powder was loaded in a corundum crucible to sinter at 1300 °C for 6 h in a reducing atmosphere. Finally the sample was cool down to room temperature naturally for

* Corresponding author.

E-mail address: jinye@cqut.edu.cn (Y. Jin).

further measurement.

2.2. Measurements and characterization

The crystal structure and phase purity of the phosphors samples were identified by using X-ray diffraction (XRD) at a Bruker D8 diffractometer with Cu K α ($\lambda = 1.54078 \text{ \AA}$). The Rietveld analysis was performed using the General Structure Analysis System (GSAS) software. PL emission and excitation were recorded on a Hitachi F-4600 fluorescence spectrophotometer equipped with a 150 W Xe-arc lamp as the excitation source. The temperature-dependent photoluminescence spectra were measured on the identical spectrophotometer attached with a self-made heating attachment and a computer controlled electric furnace.

3. Results and discussion

3.1. Phase identification and crystal structure

Fig. 1 shows the Rietveld structure refinement results of Ba $_2$ Gd $_2$ Si $_4$ O $_{13}$:0.06Ce $^{3+}$ and the refinement employed the Rietveld method in GSAS [14]. The red solid line and black crosses are calculated patterns and experimental patterns, respectively. The green line is the background and the pink short vertical lines are the position of Bragg reflections of the calculated pattern. The difference between the experimental and the calculated patterns is plotted by blue line at the bottom. Table 1 gives the structural refinement results of Ba $_2$ Gd $_2$ Si $_4$ O $_{13}$:0.06Ce $^{3+}$. The refinement data $\chi^2 = 1.652$, Rp = 4.59%, Rwp = 5.95% indicate that all the observed peaks satisfy the reflection conditions. According to the refinement results, the compound has a cubic unit cell with cell parameters $a = 12.9007 \text{ \AA}$, $b = 5.2109 \text{ \AA}$, $c = 17.5433 \text{ \AA}$, $\alpha = \gamma = 90^\circ$, $\beta = 104.069^\circ$, $V = 1143.982 \text{ \AA}^3$, $Z = 4$ and a space group of C12/c1 (15). Insert Figure demonstrates the unit cell structure of Ba $_2$ Gd $_2$ Si $_4$ O $_{13}$ and the coordination environments of Ba and Gd atoms, namely [9 + 1]-coordinated Ba $^{2+}$ and seven-coordinated Gd $^{3+}$. The ionic radii of Ce $^{3+}$ ($r = 1.07 \text{ \AA}$ when CN = 7, $r = 1.25 \text{ \AA}$ when CN = 10) are close to those of Ba $^{2+}$ ($r = 1.52 \text{ \AA}$ when CN = 10) and Gd $^{3+}$ ($r = 1.000 \text{ \AA}$ when CN = 7). Peng et al. reported that an acceptable percentage difference between doped and substituted ions do not exceed 30% [15]. The radius percentage difference

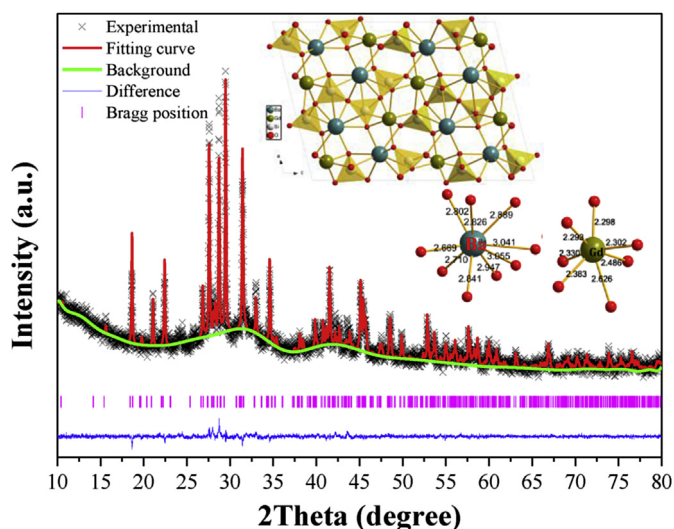


Fig. 1. (a) Rietveld refinement of Ba $_2$ Gd $_2$ Si $_4$ O $_{13}$:0.06Ce $^{3+}$ phosphor ($R_{wp} = 5.95\%$, $R_p = 4.59\%$ and $\chi^2 = 1.652$); Insert: crystal structure of Ba $_2$ Gd $_2$ Si $_4$ O $_{13}$.

Table 1
Refined structure parameters of Ba $_2$ Gd $_2$ Si $_4$ O $_{13}$:Ce $^{3+}$.

Atom	Wyck.	x	y	z	Frac.	U $_{iso}$
Ba	8f	0.1610 (14)	0.5019 (23)	0.3332 (10)	1	0.00478
Gd	8f	0.1095 (71)	0.4748 (25)	0.0855 (39)	1	0.03064
Si1	8f	0.0779 (40)	-0.0737 (56)	0.1779 (22)	1	-0.05595
Si2	8f	-0.1161 (35)	-0.0648 (08)	0.0509 (75)	1	-0.03582
O1	8f	-0.2041 (74)	-1.0395 (46)	0.1218 (07)	1	-0.00452
O2	8f	0.1026 (54)	0.2708 (14)	0.1910 (66)	1	-0.02604
O3	4e	0	-1.2252 (68)	0.25	1	0.8
O4	8f	-0.1027 (47)	1.0985 (88)	-0.0067 (21)	1	-0.0213
O5	8f	0.0597 (93)	-1.6125 (24)	0.1363 (60)	1	-0.09
O6	8f	-0.0953 (99)	-0.0308 (59)	0.1353 (85)	1	0.19639

between Ce $^{3+}$ and the possible substituted ions (Ba $^{2+}$, Gd $^{3+}$) can be calculated using the following formula:

$$Dr = 100\% \times [R_m(\text{CN}) - R_d(\text{CN})]/R_m(\text{CN})$$

where Dr is the radius percentage difference; CN is the coordinate number of the cations; R $_m$ (CN) is the radius of the possible substituted ions (Ba $^{2+}$, Gd $^{3+}$) and R $_d$ (CN) is the radius of the doped ions (Ce $^{3+}$). The Dr is 6.5% for Gd $^{3+}$ and 17.7% for Ba $^{2+}$, respectively. Therefore, it is possible for the Ce $^{3+}$ ion to substitute for both Gd $^{3+}$ and Ba $^{2+}$ in the Ba $_2$ Gd $_2$ Si $_4$ O $_{13}$ host lattice, while Gd $^{3+}$ ions have better chances considering the radii and the charge balance.

3.2. Luminescence properties of Ba $_2$ Gd $_2$ Si $_4$ O $_{13}$:Ce $^{3+}$

PLE and PL spectra of Ba $_2$ Gd $_2$ Si $_4$ O $_{13}$:Ce $^{3+}$ phosphors are shown in Fig. 2a. The excitation spectra of Ce $^{3+}$ doped powder consist of three bands with maximum at 329 nm, 310 nm and 270 nm, assigned to the Ce $^{3+}$ $^2F_{7/2}$ -5d transition. Meanwhile, an odd sharp line peaking at 272 nm is ascribed to the $^5S_{7/2}$ - 6I_1 transition of Gd $^{3+}$ [16]. In addition, within the emission spectra of Ce $^{3+}$ doped sample, the UV excitation at 329 nm leads to a broad asymmetric emission band peaking at 396 nm. The asymmetry band can be deconvoluted into two Gaussian profiles centering at 387 nm (25839 cm $^{-1}$) and 417 nm (23980 cm $^{-1}$) with an energy difference of about 1859 cm $^{-1}$ (Fig. 2b), which is attributed to the parity-allowed transitions of the lowest component of the 5d state to $^2F_{5/2}$ and $^2F_{7/2}$ levels of Ce $^{3+}$ [1,11] for its energy difference is fairly well in agreement with the theoretical difference between the $^2F_{5/2}$ and $^2F_{7/2}$ levels of Ce $^{3+}$ (~2000 cm $^{-1}$).

The PLE and PL spectra of Ba $_2$ Gd $_2$ Si $_4$ O $_{13}$:xCe $^{3+}$ ($x = 0.01, 0.02, 0.04, 0.06$ and 0.07) are shown in Fig. 3. The excitation spectra consist of three bands at 329 nm, 310 nm and 270 nm, assigned to the Ce $^{3+}$ $^2F_{7/2}$ -5d transition. Meanwhile, an odd sharp line peaking at 272 nm is ascribed to the $^5S_{7/2}$ - 6I_1 transition of Gd $^{3+}$ [16]. A broad emission band peaking at 396 nm is detected under the 329 nm excitation. The intensity of Ce $^{3+}$ emission improves from 1% to 6%, while the intensity decreases when Ce $^{3+}$ further increases due to concentration quenching. The concentration quenching is caused by energy transfer between Ce $^{3+}$ ions. According to Blasse's theory [17,18], the critical distance R $_c$ is obtained approximately by the equation:

$$R_c \approx 2 \left[\frac{3V}{4\pi x_c N} \right]^{1/3} \quad (1)$$

where x_c is the critical concentration, V is the volume of the unit cell, N is the number of Ce $^{3+}$ ions in the Ba $_2$ Gd $_2$ Si $_4$ O $_{13}$ unit cell. Here, $x_c = 0.06$, $V = 1144.1 \text{ \AA}^3$, $N = 8$ [13]. So the critical distance for Ce $^{3+}$ in Ba $_2$ Gd $_2$ Si $_4$ O $_{13}$:Ce $^{3+}$ is to be 16.56 \AA . Blasse et al. reported that the exchange interaction takes place when the R $_c$ is shorter than 5 \AA

Download English Version:

<https://daneshyari.com/en/article/1605506>

Download Persian Version:

<https://daneshyari.com/article/1605506>

[Daneshyari.com](https://daneshyari.com)